Measurement of Long-Range Angular Correlation and Quadrupole Anisotropy of Pions and (Anti)Protons in Central d + Au Collisions at $\sqrt{s_{NN}} = 200$ GeV

A. Adare,[13] C. Aidala,[38,42,43] N. N. Ajitanand,[61] Y. Akiba,[56,57] R. Akimoto,[12] H. Al-Bataineh,[50] H. Al-Ta'ani,[50] J. Alexander,[61] K. R. Andrews,[1] A. Angerami,[14] K. Aoki,[34,56] N. Apadula,[62] E. Appelt,[66] Y. Aramaki,[12,56] R. Armendariz,[8] E. C. Aschenauer,[7] E. T. Atomssa,[35] R. Averbeck,[62] T. C. Awes,[52] B. Azmoun,[7] V. Babintsev,[24] M. Bai,[6] G. Baksay,[19] L. Baksay,[19] B. Bannier,[62] K. N. Barish,[8] B. Bassalleck,[49] A. T. Basye,[1] S. Bathe,[5,8,57] V. Baublis,[55] C. Baumann,[44] A. Bazilevsky,[7] S. Belikov,[7,*] R. Belmont,[43,66] J. Ben-Benjamin,[45] R. Bennett,[62] J. H. Bhom,[70] D. S. Blau,[33] J. S. Bok,[50,70] K. Boyle,[57,62] M. L. Brooks,[38] D. Broxmeyer,[45] H. Buesching,[7] V. Bumazhnov,[24] G. Bunce,[7,57] S. Butsyk,[38] S. Campbell,[62] A. Caringi,[45] P. Castera,[62] C.-H. Chen,[62] C. Y. Chi,[14] M. Chiu,[7] I. J. Choi,[25,70] J. B. Choi,[10] R. K. Choudhury,[4] P. Christiansen,[40] T. Chujo,[65] P. Chung,[61] O. Chvala,[8] V. Cianciolo,[52] Z. Citron,[62] B. A. Cole,[14] Z. Conesa del Valle,[35] M. Connors,[62] M. Csanád,[17] T. Csörgő,[69] T. Dahms,[62] S. Dairaku,[34,56] I. Danchev,[66] K. Das,[20] A. Datta,[42] G. David,[7] M. K. Dayananda,[21] A. Denisov,[24] A. Deshpande,[57,62] E. J. Desmond,[7] K. V. Dharmawardane,[50] O. Dietzsch,[59] A. Dion,[28,62] M. Donadelli,[59] O. Drapier,[35] A. Drees,[62] K. A. Drees,[6] J. M. Durham,[38,62] A. Durum,[24] D. Dutta,[4] L. D'Orazio,[41] S. Edwards,[20] Y. V. Efremenko,[52] F. Ellinghaus,[13] T. Engelmore,[14] A. Enokizono,[52] H. En'yo,[56,57] S. Esumi,[65] B. Fadem,[45] D. E. Fields,[49] M. Finger,[9] M. Finger, Jr.,[9] F. Fleuret,[35] S. L. Fokin,[33] Z. Fraenkel,[68,*] J. E. Frantz,[51,62] A. Franz,[7] A. D. Frawley,[20] K. Fujiwara,[56] Y. Fukao,[56] T. Fusayasu,[47] C. Gal,[62] I. Garishvili,[63] A. Glenn,[37] H. Gong,[62] X. Gong,[61] M. Gonin,[35] Y. Goto,[56,57] R. Granier de Cassagnac,[35] N. Grau,[2,14] S. V. Greene,[66] G. Grim,[38] M. Grosse Perdekamp,[25] T. Gunji,[12] L. Guo,[38] H.-Å. Gustafsson,[40,*] J. S. Haggerty,[7] K. I. Hahn,[18] H. Hamagaki,[12] J. Hamblen,[63] R. Han,[54] J. Hanks,[14] C. Harper,[45] K. Hashimoto,[56,58] E. Haslum,[40] R. Hayano,[12] X. He,[21] M. Heffner,[37] T. K. Hemmick,[62] T. Hester,[8] J. C. Hill,[28] M. Hohlmann,[19] R. S. Hollis,[8] W. Holzmann,[14] K. Homma,[23] B. Hong,[32] T. Horaguchi,[23,65] Y. Hori,[12] D. Hornback,[52,63] S. Huang,[66] T. Ichihara,[56,57] R. Ichimiya,[56] H. Iinuma,[31] Y. Ikeda,[65] K. Imai,[29,34,56] M. Inaba,[65] A. Iordanova,[8] D. Isenhower,[1] M. Ishihara,[56] M. Issah,[66] D. Ivanischev,[55] Y. Iwanaga,[23] B. V. Jacak,[62] J. Jia,[7,61] X. Jiang,[38] J. Jin,[14] D. John,[63] B. M. Johnson,[7] T. Jones,[1] K. S. Joo,[46] D. Jouan,[53] D. S. Jumper,[1] F. Kajihara,[12] J. Kamin,[62] S. Kaneti,[62] B. H. Kang,[22] J. H. Kang,[70] J. S. Kang,[22] J. Kapustinsky,[38] K. Karatsu,[34,56] M. Kasai,[56,58] D. Kawall,[42,57] M. Kawashima,[56,58] A. V. Kazantsev,[33] T. Kempel,[28] A. Khanzadeev,[55] K. M. Kijima,[23] J. Kikuchi,[67] A. Kim,[18] B. I. Kim,[32] D. J. Kim,[30] E.-J. Kim,[10] Y.-J. Kim,[25] Y. K. Kim,[22] E. Kinney,[13] Á. Kiss,[17] E. Kistenev,[7] D. Kleinjan,[8] P. Kline,[62] L. Kochenda,[55] B. Komkov,[55] M. Konno,[65] J. Koster,[25] D. Kotov,[55] A. Král,[15] A. Kravitz,[14] G. J. Kunde,[38] K. Kurita,[56,58] M. Kurosawa,[56] Y. Kwon,[70] G. S. Kyle,[50] R. Lacey,[61] Y. S. Lai,[14] J. G. Lajoie,[28] A. Lebedev,[28] D. M. Lee,[38] J. Lee,[18] K. B. Lee,[32] K. S. Lee,[32] S. H. Lee,[62] S. R. Lee,[10] M. J. Leitch,[38] M. A. L. Leite,[59] X. Li,[11] P. Lichtenwalner,[45] P. Liebing,[57] S. H. Lim,[70] L. A. Linden Levy,[13] T. Liška,[15] H. Liu,[38] M. X. Liu,[38] B. Love,[66] D. Lynch,[7] C. F. Maguire,[66] Y. I. Makdisi,[6] M. D. Malik,[49] A. Manion,[62] V. I. Manko,[33] E. Mannel,[14] Y. Mao,[54,56] H. Masui,[65] F. Matathias,[14] M. McCumber,[13,62] P. L. McGaughey,[38] D. McGlinchey,[13,20] C. McKinney,[25] N. Means,[62] M. Mendoza,[8] B. Meredith,[25] Y. Miake,[65] T. Mibe,[31] A. C. Mignerey,[41] K. Miki,[56,65] A. Milov,[7,68] J. T. Mitchell,[7] Y. Miyachi,[56,64] A. K. Mohanty,[4] H. J. Moon,[46] Y. Morino,[12] A. Morreale,[8] D. P. Morrison,[7,†] S. Motschwiller,[45] T. V. Moukhanova,[33] T. Murakami,[34] J. Murata,[56,58] S. Nagamiya,[31,56] J. L. Nagle,[13,‡] M. Naglis,[68] M. I. Nagy,[69] I. Nakagawa,[56,57] Y. Nakamiya,[23] K. R. Nakamura,[34,56] T. Nakamura,[56] K. Nakano,[56] S. Nam,[18] J. Newby,[37] M. Nguyen,[62] M. Nihashi,[23] R. Nouicer,[7] A. S. Nyanin,[33] C. Oakley,[21] E. O'Brien,[7] S. X. Oda,[12] C. A. Ogilvie,[28] M. Oka,[65] K. Okada,[57] Y. Onuki,[56] A. Oskarsson,[40] M. Ouchida,[23,56] K. Ozawa,[12] R. Pak,[7] V. Pantuev,[26,62] V. Papavassiliou,[50] B. H. Park,[22] I. H. Park,[18] S. K. Park,[32] W. J. Park,[32] S. F. Pate,[50] L. Patel,[21] H. Pei,[28] J.-C. Peng,[25] H. Pereira,[16] D.Yu. Peressounko,[33] R. Petti,[7,62] C. Pinkenburg,[7] R. P. Pisani,[7] M. Proissl,[62] M. L. Purschke,[7] H. Qu,[21] J. Rak,[30] I. Ravinovich,[68] K. F. Read,[52,63] S. Rembeczki,[19] K. Reygers,[44] V. Riabov,[48,55] Y. Riabov,[55] E. Richardson,[41] D. Roach,[66] G. Roche,[39] S. D. Rolnick,[8] M. Rosati,[28] C. A. Rosen,[13] S. S. E. Rosendahl,[40] P. Ružička,[27] B. Sahlmueller,[44,62] N. Saito,[31] T. Sakaguchi,[7] K. Sakashita,[56,64] V. Samsonov,[48,55] S. Sano,[12,67] M. Sarsour,[21] T. Sato,[65] M. Savastio,[62] S. Sawada,[31] K. Sedgwick,[8] J. Seele,[13] R. Seidl,[25,57] R. Seto,[8] D. Sharma,[68] I. Shein,[24] T.-A. Shibata,[56,64] K. Shigaki,[23] H. H. Shim,[32] M. Shimomura,[65] K. Shoji,[34,56] P. Shukla,[4] A. Sickles,[7] C. L. Silva,[28] D. Silvermyr,[52] C. Silvestre,[16] K. S. Sim,[32] B. K. Singh,[3] C. P. Singh,[3] V. Singh,[3] M. Slunečka,[9] T. Sodre,[45] R. A. Soltz,[37] W. E. Sondheim,[38] S. P. Sorensen,[63] I. V. Sourikova,[7] P. W. Stankus,[52] E. Stenlund,[40] S. P. Stoll,[7] T. Sugitate,[23] A. Sukhanov,[7] J. Sun,[62] J. Sziklai,[69] E. M. Takagui,[59] A. Takahara,[12] A. Taketani,[56,57] R. Tanabe,[65] Y. Tanaka,[47] S. Taneja,[62] K. Tanida,[34,56,57,60] M. J. Tannenbaum,[7] S. Tarafdar,[3] A. Taranenko,[48,61] E. Tennant,[50] H. Themann,[62] D. Thomas,[1] T. L. Thomas,[49] M. Togawa,[57] A. Toia,[62] L. Tomášek,[27] M. Tomášek,[27] H. Torii,[23] R. S. Towell,[1] I. Tserruya,[68] Y. Tsuchimoto,[23]

0031-9007/15/114(19)/192301(8)

K. Utsunomiya,[12] C. Vale,[7] H. Valle,[66] H. W. van Hecke,[38] E. Vazquez-Zambrano,[14] A. Veicht,[14,25] J. Velkovska,[66] R. Vértesi,[69] M. Virius,[15] A. Vossen,[25] V. Vrba,[27] E. Vznuzdaev,[55] X. R. Wang,[50] D. Watanabe,[23] K. Watanabe,[65] Y. Watanabe,[56,57] Y. S. Watanabe,[12] F. Wei,[28] R. Wei,[61] J. Wessels,[44] S. N. White,[7] D. Winter,[14] C. L. Woody,[7] R. M. Wright,[1] M. Wysocki,[13] Y. L. Yamaguchi,[12,56] K. Yamaura,[23] R. Yang,[25] A. Yanovich,[24] J. Ying,[21] S. Yokkaichi,[56,57] J. S. Yoo,[18] Z. You,[38,54] G. R. Young,[52] I. Younus,[36,49] I. E. Yushmanov,[33] W. A. Zajc,[14] A. Zelenski,[6] and S. Zhou[11]

(PHENIX Collaboration)

[1]*Abilene Christian University, Abilene, Texas 79699, USA*
[2]*Department of Physics, Augustana College, Sioux Falls, South Dakota 57197, USA*
[3]*Department of Physics, Banaras Hindu University, Varanasi 221005, India*
[4]*Bhabha Atomic Research Centre, Bombay 400 085, India*
[5]*Baruch College, City University of New York, New York, New York 10010, USA*
[6]*Collider-Accelerator Department, Brookhaven National Laboratory, Upton, New York 11973-5000, USA*
[7]*Physics Department, Brookhaven National Laboratory, Upton, New York 11973-5000, USA*
[8]*University of California–Riverside, Riverside, California 92521, USA*
[9]*Charles University, Ovocný trh 5, Praha 1, 116 36 Prague, Czech Republic*
[10]*Chonbuk National University, Jeonju 561-756, Korea*
[11]*Science and Technology on Nuclear Data Laboratory, China Institute of Atomic Energy, Beijing 102413, People's Republic of China*
[12]*Center for Nuclear Study, Graduate School of Science, University of Tokyo, 7-3-1 Hongo, Bunkyo, Tokyo 113-0033, Japan*
[13]*University of Colorado, Boulder, Colorado 80309, USA*
[14]*Columbia University, New York, New York 10027, USA and Nevis Laboratories, Irvington, New York 10533, USA*
[15]*Czech Technical University, Zikova 4, 166 36 Prague 6, Czech Republic*
[16]*Dapnia, CEA Saclay, F-91191 Gif-sur-Yvette, France*
[17]*ELTE, Eötvös Loránd University, H- 1117 Budapest, Pázmány P. s. 1/A, Hungary*
[18]*Ewha Womans University, Seoul 120-750, Korea*
[19]*Florida Institute of Technology, Melbourne, Florida 32901, USA*
[20]*Florida State University, Tallahassee, Florida 32306, USA*
[21]*Georgia State University, Atlanta, Georgia 30303, USA*
[22]*Hanyang University, Seoul 133-792, Korea*
[23]*Hiroshima University, Kagamiyama, Higashi-Hiroshima 739-8526, Japan*
[24]*IHEP Protvino, State Research Center of Russian Federation, Institute for High Energy Physics, Protvino 142281, Russia*
[25]*University of Illinois at Urbana-Champaign, Urbana, Illinois 61801, USA*
[26]*Institute for Nuclear Research of the Russian Academy of Sciences, prospekt 60-letiya Oktyabrya 7a, Moscow 117312, Russia*
[27]*Institute of Physics, Academy of Sciences of the Czech Republic, Na Slovance 2, 182 21 Prague 8, Czech Republic*
[28]*Iowa State University, Ames, Iowa 50011, USA*
[29]*Advanced Science Research Center, Japan Atomic Energy Agency, 2-4 Shirakata Shirane, Tokai-mura, Naka-gun, Ibaraki-ken 319-1195, Japan*
[30]*Helsinki Institute of Physics and University of Jyväskylä, P.O. Box 35, FI-40014 Jyväskylä, Finland*
[31]*KEK, High Energy Accelerator Research Organization, Tsukuba, Ibaraki 305-0801, Japan*
[32]*Korea University, Seoul 136-701, Korea*
[33]*Russian Research Center "Kurchatov Institute," Moscow 123098, Russia*
[34]*Kyoto University, Kyoto 606-8502, Japan*
[35]*Laboratoire Leprince-Ringuet, Ecole Polytechnique, CNRS-IN2P3, Route de Saclay, F-91128 Palaiseau, France*
[36]*Physics Department, Lahore University of Management Sciences, Lahore, Pakistan*
[37]*Lawrence Livermore National Laboratory, Livermore, California 94550, USA*
[38]*Los Alamos National Laboratory, Los Alamos, New Mexico 87545, USA*
[39]*LPC, Université Blaise Pascal, CNRS-IN2P3, Clermont-Fd, 63177 Aubiere Cedex, France*
[40]*Department of Physics, Lund University, Box 118, SE-221 00 Lund, Sweden*
[41]*University of Maryland, College Park, Maryland 20742, USA*
[42]*Department of Physics, University of Massachusetts, Amherst, Massachusetts 01003-9337, USA*
[43]*Department of Physics, University of Michigan, Ann Arbor, Michigan 48109-1040, USA*
[44]*Institut fur Kernphysik, University of Muenster, D-48149 Muenster, Germany*
[45]*Muhlenberg College, Allentown, Pennsylvania 18104-5586, USA*
[46]*Myongji University, Yongin, Kyonggido 449-728, Korea*
[47]*Nagasaki Institute of Applied Science, Nagasaki-shi, Nagasaki 851-0193, Japan*
[48]*National Research Nuclear University, MEPhI, Moscow Engineering Physics Institute, Moscow, 115409, Russia*
[49]*University of New Mexico, Albuquerque, New Mexico 87131, USA*
[50]*New Mexico State University, Las Cruces, New Mexico 88003, USA*

[51]Department of Physics and Astronomy, Ohio University, Athens, Ohio 45701, USA
[52]Oak Ridge National Laboratory, Oak Ridge, Tennessee 37831, USA
[53]IPN-Orsay, Universite Paris Sud, CNRS-IN2P3, BP1, F-91406 Orsay, France
[54]Peking University, Beijing 100871, People's Republic of China
[55]PNPI, Petersburg Nuclear Physics Institute, Gatchina, Leningrad region 188300, Russia
[56]RIKEN Nishina Center for Accelerator-Based Science, Wako, Saitama 351-0198, Japan
[57]RIKEN BNL Research Center, Brookhaven National Laboratory, Upton, New York 11973-5000, USA
[58]Physics Department, Rikkyo University, 3-34-1 Nishi-Ikebukuro, Toshima, Tokyo 171-8501, Japan
[59]Universidade de São Paulo, Instituto de Física, Caixa Postal 66318, São Paulo CEP05315-970, Brazil
[60]Seoul National University, Seoul, Korea
[61]Chemistry Department, Stony Brook University, SUNY, Stony Brook, New York 11794-3400, USA
[62]Department of Physics and Astronomy, Stony Brook University, SUNY, Stony Brook, New York 11794-3800, USA
[63]University of Tennessee, Knoxville, Tennessee 37996, USA
[64]Department of Physics, Tokyo Institute of Technology, Oh-okayama, Meguro, Tokyo 152-8551, Japan
[65]Institute of Physics, University of Tsukuba, Tsukuba, Ibaraki 305, Japan
[66]Vanderbilt University, Nashville, Tennessee 37235, USA
[67]Waseda University, Advanced Research Institute for Science and Engineering, 17 Kikui-cho, Shinjuku-ku, Tokyo 162-0044, Japan
[68]Weizmann Institute, Rehovot 76100, Israel
[69]Institute for Particle and Nuclear Physics, Wigner Research Centre for Physics, Hungarian Academy of Sciences (Wigner RCP, RMKI) H-1525 Budapest 114, PO Box 49, Budapest, Hungary
[70]Yonsei University, IPAP, Seoul 120-749, Korea

(Received 30 April 2014; revised manuscript received 9 March 2015; published 12 May 2015)

We present azimuthal angular correlations between charged hadrons and energy deposited in calorimeter towers in central $d+\mathrm{Au}$ and minimum bias $p+p$ collisions at $\sqrt{s_{NN}} = 200$ GeV. The charged hadron is measured at midrapidity $|\eta| < 0.35$, and the energy is measured at large rapidity ($-3.7 < \eta < -3.1$, Au-going direction). An enhanced near-side angular correlation across $|\Delta\eta| > 2.75$ is observed in $d+\mathrm{Au}$ collisions. Using the event plane method applied to the Au-going energy distribution, we extract the anisotropy strength v_2 for inclusive charged hadrons at midrapidity up to $p_T = 4.5$ GeV/c. We also present the measurement of v_2 for identified $\pi^\pm$ and (anti)protons in central $d+\mathrm{Au}$ collisions, and observe a mass-ordering pattern similar to that seen in heavy-ion collisions. These results are compared with viscous hydrodynamic calculations and measurements from $p+\mathrm{Pb}$ at $\sqrt{s_{NN}} = 5.02$ TeV. The magnitude of the mass ordering in $d+\mathrm{Au}$ is found to be smaller than that in $p+\mathrm{Pb}$ collisions, which may indicate smaller radial flow in lower energy $d+\mathrm{Au}$ collisions.

DOI: 10.1103/PhysRevLett.114.192301 PACS numbers: 25.75.Dw

Small collision systems, $d+\mathrm{Au}$ and $p+\mathrm{Pb}$, have been studied at the Relativistic Heavy Ion Collider (RHIC) and the Large Hadron Collider (LHC) to understand baseline nuclear effects for heavy-ion collisions in which hot nuclear matter is made. The $d+\mathrm{Au}$ and $p+\mathrm{Pb}$ systems have generally been considered too small to create significant quantities of hot nuclear matter. This assumption has been challenged in $p+\mathrm{Pb}$ at $\sqrt{s_{NN}} = 5.02$ TeV with the measurements of (i) near-side azimuthal correlations across a large pseudorapidity gap [1–3], also observed in high multiplicity $p+p$ collisions at 7 TeV [4], and (ii) the elliptic anisotropy parameter v_2 measured by multiple particle correlations [5,6].

Hydrodynamic models, successfully applied to heavy-ion data at RHIC and the LHC, can qualitatively reproduce the v_2 results from $p+$ nucleus and $d+$ nucleus collisions [7–9]. If hydrodynamics is the primary cause of the observed effects, then there should be a mass ordering of the magnitudes of v_2 for identified particles, in which heavier particles have smaller v_2 values at low $p_T < 1.5$ GeV/c [10,11]. Recently, such mass ordering has been observed in $p+\mathrm{Pb}$ collisions at LHC for v_2 of $\pi^\pm$ and $p, \bar{p}$ [12]. Finite near-side correlations can also arise from enhanced two-gluon emission at high parton densities as in the color glass condensate model [13–15].

Long-range angular correlations and elliptic anisotropy of inclusive and identified hadrons in $p+p$ and $d+\mathrm{Au}$ collisions at RHIC can provide crucial tests as to whether a hydrodynamically expanding medium is created in these small systems. The v_2 in $d+\mathrm{Au}$ has been measured from hadron pair correlations, within a limited rapidity range ($0.7 > |\Delta\eta| > 0.48$) and under the assumption that jetlike correlations are the same in various multiplicity-selected events [16]. In this Letter, we report measurements of azimuthal correlations in top 5% central $d+\mathrm{Au}$ and minimum bias $p+p$ collisions between charged hadrons at midrapidity ($|\eta| < 0.35$) and energy deposited at large rapidity $-3.7 < \eta < -3.1$ (Au-going direction). We also report v_2 for inclusive hadron and identified pions and (anti)protons in $d+\mathrm{Au}$ at midrapidity using an event plane across $|\Delta\eta| > 2.75$.

The data were obtained from $p+p$ in the 2008 and 2009 experimental runs and $d+\mathrm{Au}$ in the 2008 run with the PHENIX detector. The event centrality class in $d+\mathrm{Au}$ collisions is determined as a percentile of the total charge measured in the PHENIX beam-beam counter covering $-3.9 < \eta < -3.0$ on the Au-going side [17–20]. For the 5% most central $d+\mathrm{Au}$ collisions, the corresponding number of binary collisions and number of participants are estimated by a Glauber model to be 18.1 ± 1.2 and 17.8 ± 1.2, respectively [17].

Charged particles used in this analysis are reconstructed in the two PHENIX central-arm tracking systems, consisting of drift chambers and multiwire proportional pad chambers (PC) [21]. Each arm covers $\pi/2$ in azimuth and $|\eta| < 0.35$, and the tracking system achieves a momentum resolution of $\delta p/p \approx 0.7\% \oplus 1.1\% \times p(\mathrm{GeV}/c)$.

The drift-chamber tracks are matched to hits in the third layer of the PC, reducing the contribution of tracks originating from decays and photon conversions. Hadron identification is achieved using the time-of-flight detectors, with different technologies in the east and west arms, for which the timing resolutions are 130 and 95 ps, respectively. Pions and (anti)proton tracks are identified with over 99% purity at momenta up to 3 GeV/c [18,22] in both systems.

Energy deposited at large rapidity in the Au-going direction is measured by the towers in the south-side Muon Piston Calorimeter (MPC-S) [23]. The MPC-S comprises 192 towers of $PbWO_4$ crystal covering 2π in azimuth and $-3.7 < \eta < -3.1$ in pseudorapidity, with each tower subtending approximately $\Delta\eta \times \Delta\phi \approx 0.12 \times 0.18$. Over 95% of the energy detected in the MPC is from photons, which are primarily produced in the decays of π^0 and η mesons. Photons are well localized, as each will deposit over 90% of its energy into one tower if it hits the tower's center. To avoid the background from noncollision noise sources (~75 MeV) and cut out the deposits by minimum ionization particles (~245 MeV), we select towers with deposited energy $E_{\mathrm{tower}} > 3$ GeV.

We first examine the long-range azimuthal angular correlation of pairs consisting of one track in the central arm and one tower in the MPC-S. Because the towers are mainly fired by photons, and the azimuthal extent of each energy deposition is much smaller than the size of azimuthal angular correlation from jets or elliptic flow, these track-tower pair correlations will be good proxies for hadron-photon correlations without attempting to reconstruct individual photon showers. We construct the signal distribution $S(\Delta\phi, p_T)$ of track-tower pairs over relative azimuthal angle $\Delta\phi \equiv \phi_{\mathrm{track}} - \phi_{\mathrm{tower}}$, each with weight w_{tower}, in bins of track transverse momentum p_T:

$$S(\Delta\phi, p_T) = \frac{d(w_{\mathrm{tower}} N_{\text{same event}}^{\text{track}(p_T)\text{-tower}})}{d\Delta\phi}. \qquad (1)$$

Here ϕ_{track} is the azimuth of the track as it leaves the primary vertex, ϕ_{tower} is the azimuth of the center of the calorimeter tower. The w_{tower} is chosen as the tower's transverse energy $E_T = E_{\mathrm{tower}} \sin(\theta_{\mathrm{tower}})$. Because the calorimeter is operating in a linear regime, the overall E_T pattern on each event will simply be the sum of the patterns from each impinging particle, so we expect no distortion effect due to occupancy. To correct for the nonuniform PHENIX azimuthal acceptance in the central arm tracking system, we then construct the corresponding "mixed-event" distribution $M(\Delta\phi, p_T)$ over track-tower pairs, where the tracks and tower signals are from different events in the same centrality and vertex position class. We then construct the normalized correlation function,

$$C(\Delta\phi, p_T) = \frac{S(\Delta\phi, p_T)}{M(\Delta\phi, p_T)} \frac{\int_0^{2\pi} M(\Delta\phi, p_T) d\Delta\phi}{\int_0^{2\pi} S(\Delta\phi, p_T) d\Delta\phi}, \qquad (2)$$

whose shape is proportional to the true pairs distribution over $\Delta\phi$.

Figure 1 shows the correlation functions $C(\Delta\phi, p_T)$ for different p_T bins, for the 5% most central $d+\mathrm{Au}$ collisions and for minimum bias $p+p$ collisions. Central $d+\mathrm{Au}$ collisions show a visible enhancement

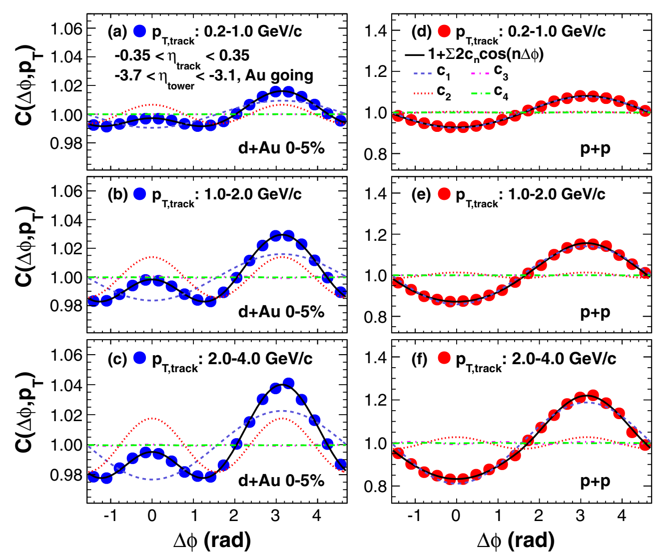

FIG. 1 (color online). The azimuthal correlation functions $C(\Delta\phi, p_T)$, as defined in Eq. (2), for track-tower pairs with different track p_T selections in (a)–(c) 0%–5% central $d+\mathrm{Au}$ collisions and (d)–(f) minimum bias $p+p$ collisions at $\sqrt{s_{NN}} = 200$ GeV. From top to bottom, the track p_T bins are (a), (d) 0.2–1.0, (b), (e) 1.0–2.0, and (c), (f) 2.0–4.0 GeV/c. The pairs are formed between charged tracks measured in the PHENIX central arms at $|\eta| < 0.35$ and towers in the MPC-S calorimeter ($-3.7 < \eta < -3.1$, Au going). A near-side peak is observed in the central $d+\mathrm{Au}$ collisions which is not seen in minimum bias $p+p$ collisions. Each correlation function is fit with a four-term Fourier cosine expansion; the individual components $n=1$ to $n=4$ are drawn on each panel, together with the fit function sum.

of near-side pairs, producing a local maximum in the distribution at $\Delta\phi \sim 0$, which is not seen in the $p+p$ data. We analyze the distributions by fitting each $C(\Delta\phi, p_T)$ to a four-term Fourier cosine expansion, $f(\Delta\phi) = 1 + \sum_{n=1}^{4} 2c_n(p_T)\cos(n\Delta\phi)$; the sum function and each individual cosine component are plotted in Fig. 1 for each distribution. We observe that the $p+p$ distribution shape is described almost entirely by the dipole term $\cos(\Delta\phi)$, as expected generically by transverse momentum conservation, via processes such as dijet production or soft string fragmentation; the shape in central $d+\mathrm{Au}$ collisions exhibits both dipole and quadrupole $\cos(2\Delta\phi)$ terms with similar magnitudes. Both c_3 and c_4 are found to be ≈ 0, as shown in Fig. 1.

Figure 2 shows the fitted c_2 parameters from the $d+\mathrm{Au}$ and $p+p$ collisions with both statistical and systematic uncertainties. We estimate contributions to systematic uncertainties from two main sources: (1) tracking backgrounds from weak decays and photon conversions and (2) multiple collisions in a bunch crossing (pileup) in $d+\mathrm{Au}$ collisions. We estimate the tracking background contribution by reducing the spatial matching windows in the third layer of the PC from 3σ to 2σ, and find that the change is less than 2% fractionally in c_2. To study the pile-up effect in $d+\mathrm{Au}$ collisions, we separate the $d+\mathrm{Au}$ data set into two groups, one from a period with lower luminosity and the other with the higher luminosity. The corresponding pile-up event fractions in central $d+\mathrm{Au}$ collisions are 3.5% and 7.0%, respectively. The $c_2^{d+\mathrm{Au}}$ in the lower luminosity data set is around 5% higher than that in higher luminosity across all p_T. The average pile-up fraction for the total data sample is around 4%–5% and a systematic uncertainty around 10% is assigned to cover this effect. Additionally, we compare c_2^{p+p} results for $p+p$ data taken in the 2008 and 2009 running periods, and see a difference of less than 5% for $p_T < 1$ GeV/c, increasing to 15% for $p_T > 3$ GeV/c. To characterize biases that might arise because the tower energy and centrality are measured in the same rapidity range, we have compared results obtained using two different detectors in the Au-going direction to define the event centrality: (i) the reaction-plane detector ($-2.8 < \eta < -1.0$) [24] and (ii) the zero-degree calorimeter ($\eta < -6.5$) [25]. The c_2 values obtained in the two cases differ by 6% from those reported here.

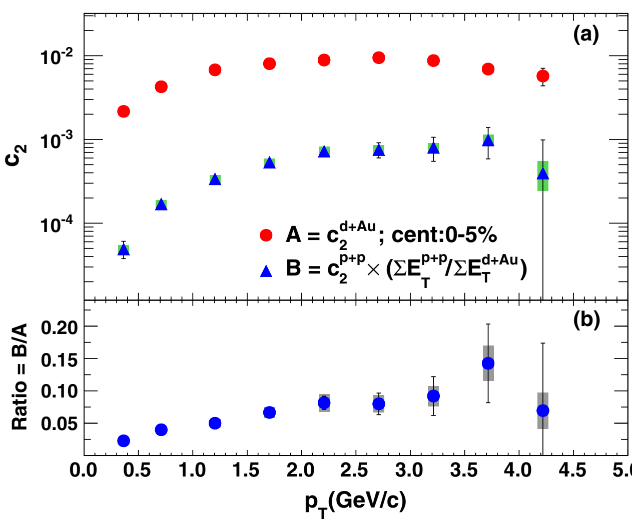

FIG. 2 (color online). (a) $c_2(p_T)$ for track-tower pairs from 0%–5% $d+\mathrm{Au}$ collisions and $c_2(p_T)$ for pairs in minimum bias $p+p$ collisions times the dilution factor $(\Sigma E_T{}^{p+p}/\Sigma E_T{}^{d+\mathrm{Au}})$. Panel (b) shows their ratio, indicating that the contribution to the c_2 amplitude in $d+\mathrm{Au}$ from elementary processes present in $p+p$ is small, only a few percent at low p_T and rising to only 10% by 4.5 GeV/c. Both statistical (bar) and systematic (band) uncertainties are shown.

Some portion of the correlation quadrupole strength c_2 in the $d+\mathrm{Au}$ data could be due to elementary processes such as dijet fragmentation (mainly from the away side) and resonance decays. We can estimate the effect of such processes under the assumptions that (i) all correlations present in minimum bias $p+p$ collisions are due to elementary processes and (ii) those same processes occur in the measured $d+\mathrm{Au}$ system as a simple superposition of several nucleon-nucleon collisions. In this case, we would expect the contribution from elementary processes to be equal to the $c_2^{p+p}(p_T)$ but diluted by the increase in particle multiplicity between $p+p$ and $d+\mathrm{Au}$ collisions, if the number of elementary processes is proportional to the multiplicity of the other particle used in pair correlations (see also the "scalar product method," as in Refs. [26,27]). We estimate the ratio of the $p+p$ to $d+\mathrm{Au}$ general multiplicities by measuring the ratio of the total transverse energy $\sum E_T$ seen in the MPC-S calorimeter in $p+p$ versus $d+\mathrm{Au}$ events, which we find to be approximately $1/(17.9 \pm 0.35)$ and only weakly dependent on the track p_T ($\leq 2\%$). We can then separate $c_2^{d+\mathrm{Au}}(p_T)$ into elementary and nonelementary components:

$$c_2^{d+\mathrm{Au}}(p_T) = c_2^{\mathrm{nonelem}}(p_T) + c_2^{\mathrm{elem}}(p_T) \approx c_2^{\mathrm{nonelem}}(p_T) + c_2^{p+p}(p_T)\frac{\Sigma E_T^{p+p}}{\Sigma E_T^{d+\mathrm{Au}}}. \quad (3)$$

The ratio in Fig. 2(b) shows that the contribution to $c_2^{d+\mathrm{Au}}$ from elementary processes is indeed small, ranging from a few percent at the lowest p_T to around 10% at the highest p_T, and no more than 13% with the other centrality selections mentioned above. The presence of the near-side peak in the pairs distribution in the central $d+\mathrm{Au}$ system is reproduced in some physics model calculations. The formation of a medium that evolves hydrodynamically is one such possibility [7–9], but processes such as initial state gluon saturation [14,15] could also create such an effect.

To quantitatively address the physics of this near-side peak and compare with detailed hydrodynamics calculations, the v_2 of charged hadrons, pions, and (anti)protons at midrapidity is measured via the event plane method [28].

The v_2 is measured as $v_2(p_T) = \langle \cos 2(\phi^{\rm particle} - \Psi_2^{\rm obs})\rangle / {\rm Res}(\Psi_2^{\rm obs})$, where the average is over particles in the p_T bin and over events. The second order event plane direction $\Psi_2^{\rm obs}$ is determined using the MPC-S (Au going). The study of correlation strength as above indicates that the elementary-process contribution to the event plane v_2 result is similarly small, less than 10% fractionally out to $p_T = 4.5$ GeV/c. The event plane resolution ${\rm Res}(\Psi_2^{\rm obs})$ ($\sim 0.151 \pm 0.003$) is calculated through the standard three subevents method [28,29], with the other two event planes being (i) the second order event plane determined from central-arm tracks, restricted to low p_T ($0.2 < p_T < 2.0$ GeV/c) to minimize contribution from jet fragments, and (ii) the first order event plane measured with spectator neutrons in the shower-maximum detector on the Au-going side ($\eta < -6.5$) [25,29]. The systematic uncertainties on the v_2 of charged hadrons are mainly from the tracking background (2%) and pile-up effects (5%), as described above, and also from the difference in v_2 from different event plane determinations. To estimate the systematic uncertainty of the latter, we compare the v_2 extracted with the MPC-S event plane with that using the south (Au-going) beam-beam counter, and the two measurements of v_2 are consistent to within 5%. The difference for v_2 from the different centrality determinations as discussed previously is less than 3%.

The v_2 of charged hadrons for 0%–5% central d + Au events with event plane methods are shown in Fig. 3(a) as $v_2(EP)$ for p_T up to 4.5 GeV/c, along with a polynomial fit through the points. Also shown are our earlier measurement with two particle correlations [$v_2(2p)$] and the v_2 measured in the central p + Pb collisions at LHC. Figure 3(b) shows the ratios of all of these measurements divided by the fitting results. The v_2 from our prior measurements, with subtraction of peripheral data to reduce jet contributions, exceed the current measurement; differences range from about 15% at $p_T = 1.0$ GeV/c to about 50% at $p_T = 2.2$ GeV/c. The difference is about 1.5σ for the top three points with the largest deviations from the fit. It may be due to different jetlike correlation being present in central and peripheral collisions [30]. The present measurement, without peripheral subtraction, is performed with $|\Delta\eta| > 2.75$, far away from the near-side main jet peak. The contribution from jet, which includes both near and away side, has been found to be less than 10% from the study of c_2 shown in Fig. 2. Even if there is a 30% enhancement of jetlike correlation from $p + p$ to central d + Au collisions, it will only raise from 10% to 13% our estimate of the jetlike contribution to the v_2 in central d + Au collisions. The present v_2 measurement is closer to that of p + Pb collisions [2,3,6]. It is about 20% higher than that of p + Pb at $p_T = 1$ GeV/c, and the difference decreases to a few percent at $p_T > 2.0$ GeV/c.

Figure 4 shows the midrapidity $v_2(p_T)$ for identified charged pions and (anti)protons, with charge signs combined for each species, up to $p_T = 3$ GeV/c using the event plane method; the systematic uncertainties are the same as for inclusive charged hadrons. A distinctive mass splitting can be seen. The pion v_2 is higher than the proton's for $p_T < 1.5$ GeV/c, as has been seen universally in heavy-ion collisions at RHIC [34–39]. Figure 4(a) also shows calculations of viscous hydrodynamics with Glauber initial conditions starting at $\tau = 0.5$ fm/c with $\eta/s = 1.0/(4\pi)$, followed by a hadronic cascade [31–33].

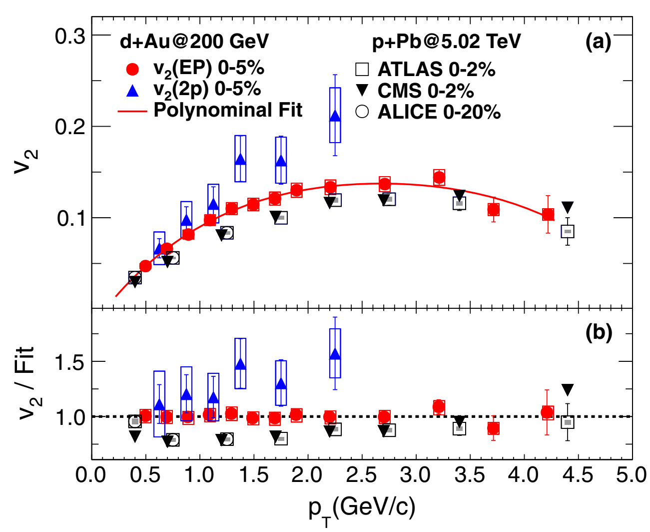

FIG. 3 (color online). Measured $v_2(EP)$ for midrapidity charged tracks in 0%–5% central d + Au at $\sqrt{s_{NN}} = 200$ GeV using the event plane method in (a). Also shown are v_2 measured in central p + Pb collisions at $\sqrt{s_{NN}} = 5.02$ TeV [2,3,6] and our prior measurements with two particle correlations [$v_2(2p)$] for d + Au collisions [16]. A polynomial fit to the current measurement and the ratios of experimental values to the fit are shown in (b).

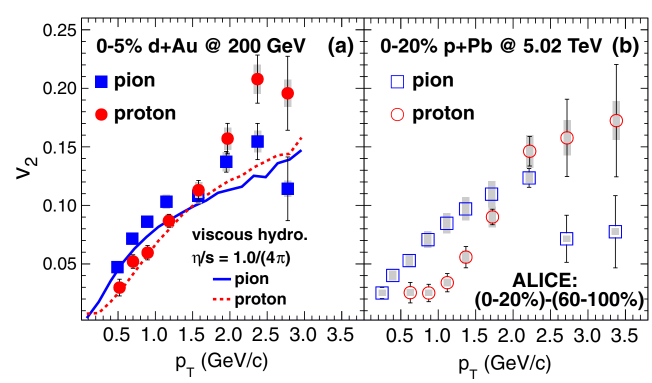

FIG. 4 (color online). Measured $v_2(p_T)$ for identified pions and (anti)protons, each charged combined, in 0%–5% central d + Au collisions at RHIC. In (a) the data are compared with the calculation from a viscous hydrodynamic model [31–33], and in (b) the v_2 data for pions and protons in 0%–20% central p + Pb collisions at LHC are shown for comparison [12], they are measured from pair correlations with a peripheral event yield subtraction.

The splitting at lower p_T is also seen in the calculation. The identified particle v_2 in 0%–20% $p+\mathrm{Pb}$ collisions are shown in Fig. 4(b) for comparison [12]. The magnitude of the mass splitting in RHIC $d+\mathrm{Au}$ is smaller than that seen in LHC $p+\mathrm{Pb}$, which could be an indicator of stronger radial flow in the higher energy collisions [40].

We have presented measurements of long-range azimuthal correlations between particles at midrapidity and at backward rapidity (Au-going direction) in 0%–5% central $d+\mathrm{Au}$ collisions at $\sqrt{s_{NN}} = 200$ GeV. We find a localized near-side azimuthal angular correlation in these collisions for pairs across $|\Delta\eta| > 2.75$ which is not apparent in minimum bias $p+p$ collisions at the same collision energy. The anisotropy strength v_2 is measured for midrapidity particles with respect to an event plane determined from a region separated by the same pseudorapidity interval. The v_2 values are qualitatively similar to those observed in central $p+\mathrm{Pb}$ collisions at $\sqrt{s_{NN}} = 5.02$ TeV. The v_2 for identified pions and (anti) protons at midrapidity exhibit a mass ordering, qualitatively similar to observations in relativistic heavy-ion collisions. This ordering can be described by a viscous hydrodynamic model, where they are believed to reflect radial flow in hydrodynamics. The magnitude of mass splitting in $v_2(p_t)$ is found to be smaller in $d+\mathrm{Au}$ collisions in comparison to $p+\mathrm{Pb}$ collisions at higher energies, possibly indicating smaller radial flow in $d+\mathrm{Au}$ at $\sqrt{s_{NN}} = 200$ GeV.

We thank the staff of the Collider-Accelerator and Physics Departments at Brookhaven National Laboratory and the staff of the other PHENIX participating institutions for their vital contributions. We acknowledge support from the Office of Nuclear Physics in the Office of Science of the Department of Energy, the National Science Foundation, Abilene Christian University Research Council, Research Foundation of SUNY, and Dean of the College of Arts and Sciences, Vanderbilt University (U.S.), Ministry of Education, Culture, Sports, Science, and Technology and the Japan Society for the Promotion of Science (Japan), Conselho Nacional de Desenvolvimento Científico e Tecnológico and Fundação de Amparo à Pesquisa do Estado de São Paulo (Brazil), Natural Science Foundation of China (People's Republic of China), Ministry of Education, Youth and Sports (Czech Republic), Centre National de la Recherche Scientifique, Commissariat à l'Énergie Atomique, and Institut National de Physique Nucléaire et de Physique des Particules (France), Bundesministerium für Bildung und Forschung, Deutscher Akademischer Austausch Dienst, and Alexander von Humboldt Stiftung (Germany), Hungarian National Science Fund, OTKA, Károly Róbert University College (Hungary), Department of Atomic Energy and Department of Science and Technology (India), Israel Science Foundation (Israel), National Research Foundation of Korea of the Ministry of Science, ICT, and Future Planning (Korea), Physics Department, Lahore University of Management Sciences (Pakistan), Ministry of Education and Science, Russian Academy of Sciences, Federal Agency of Atomic Energy (Russia), VR and Wallenberg Foundation (Sweden), the U.S. Civilian Research and Development Foundation for the Independent States of the Former Soviet Union, the Hungarian American Enterprise Scholarship Fund, the U.S.-Hungarian Fulbright Foundation for Educational Exchange, and the U.S.-Israel Binational Science Foundation.

*Deceased.
†PHENIX Co-Spokesperson.
morrison@bnl.gov
‡PHENIX Co-Spokesperson.
jamie.nagle@colorado.edu

[1] S. Chatrchyan *et al.* (CMS Collaboration), Observation of long-range near-side angular correlations in proton-lead collisions at the LHC, Phys. Lett. B **718**, 795 (2013).

[2] G. Aad *et al.* (ATLAS Collaboration), Observation of Associated Near-Side and Away-Side Long-Range Correlations in $\sqrt{s_{NN}} = 5.02$ TeV Proton-Lead Collisions with the ATLAS Detector, Phys. Rev. Lett. **110**, 182302 (2013).

[3] B. Abelev *et al.* (ALICE Collaboration), Long-range angular correlations on the near and away side in p-Pb collisions at $\sqrt{s_{NN}} = 5.02$ TeV, Phys. Lett. B **719**, 29 (2013).

[4] V. Khachatryan *et al.* (CMS Collaboration), Observation of long-range near-side angular correlations in proton-proton collisions at the LHC, J. High Energy Phys. 09 (2010) 091.

[5] G. Aad *et al.* (ATLAS Collaboration), Measurement with the ATLAS detector of multi-particle azimuthal correlations in $p+\mathrm{Pb}$ collisions at $\sqrt{s_{NN}} = 5.02$ TeV, Phys. Lett. B **725**, 60 (2013).

[6] S. Chatrchyan *et al.* (CMS Collaboration), Multiplicity and transverse momentum dependence of two- and four-particle correlations in pPb and PbPb collisions, Phys. Lett. B **724**, 213 (2013).

[7] P. Bozek and W. Broniowski, Collective dynamics of the high-energy proton-nucleus collisions, Phys. Rev. C **88**, 014903 (2013).

[8] A. Bzdak, B. Schenke, P. Tribedy, and R. Venugopalan, Initial state geometry and the role of hydrodynamics in proton-proton, proton-nucleus, and deuteron-nucleus collisions, Phys. Rev. C **87**, 064906 (2013).

[9] G.-Y. Qin and B. Mueller, Elliptic and triangular flow anisotropy in deuteron-gold collisions at RHIC and proton-lead collisions at the LHC, Phys. Rev. C **89**, 044902 (2014).

[10] P. Huovinen, P. F. Kolb, U. Heinz, P. V. Ruuskanen, and S. A. Voloshin, Radial and elliptic flow at RHIC: Further predictions, Phys. Lett. B **503**, 58 (2001).

[11] P. Bozek, W. Broniowski, and G. Torrieri, Mass Hierarchy in Identified Particle Distributions in Proton-Lead Collisions, Phys. Rev. Lett. **111**, 172303 (2013).

[12] B. B. Abelev *et al.* (ALICE Collaboration), Long-range angular correlations of π, K and p in p-Pb collisions at $\sqrt{s_{NN}} = 5.02$ TeV, Phys. Lett. B **726**, 164 (2013).

[13] K. Dusling and R. Venugopalan, Azimuthal Collimation of Long Range Rapidity Correlations by Strong Color Fields in High Multiplicity Hadron-Hadron Collisions, Phys. Rev. Lett. **108**, 262001 (2012).

[14] K. Dusling and R. Venugopalan, Explanation of systematics of CMS $p+\mathrm{Pb}$ high-multiplicity dihadron data at $\sqrt{s_{NN}}=5.02$ TeV, Phys. Rev. D **87**, 054014 (2013).
[15] K. Dusling and R. Venugopalan, Comparison of the color glass condensate to dihadron correlations in proton-proton and proton-nucleus collisions, Phys. Rev. D **87**, 094034 (2013).
[16] A. Adare *et al.* (PHENIX Collaboration), Quadrupole Anisotropy in Dihadron Azimuthal Correlations in Central $d+\mathrm{Au}$ Collisions at $\sqrt{s_{NN}}=200$ GeV, Phys. Rev. Lett. **111**, 212301 (2013).
[17] A. Adare *et al.* (PHENIX Collaboration), Centrality categorization for $R_{p(d)+\mathrm{Au}}$ in high-energy collisions, Phys. Rev. C **90**, 034902 (2014).
[18] A. Adare *et al.* (PHENIX Collaboration), Spectra and ratios of identified particles in $\mathrm{Au}+\mathrm{Au}$ and $d+\mathrm{Au}$ collisions at $\sqrt{s_{NN}}=200$ GeV, Phys. Rev. C **88**, 024906 (2013).
[19] A. Adare *et al.* (PHENIX Collaboration), Suppression of Back-to-Back Hadron Pairs at Forward Rapidity in $d+\mathrm{Au}$ Collisions at $\sqrt{s_{NN}}=200$ GeV, Phys. Rev. Lett. **107**, 172301 (2011).
[20] A. Adare *et al.*, Nuclear Modification of ψ', χ_c, and J/ψ Production in $d+\mathrm{Au}$ Collisions at $\sqrt{s_{NN}}=200$ GeV, Phys. Rev. Lett. **111**, 202301 (2013).
[21] K. Adcox *et al.* (PHENIX Collaboration), PHENIX central arm tracking detectors, Nucl. Instrum. Methods Phys. Res., Sect. A **499**, 489 (2003).
[22] A. Adare *et al.* (PHENIX Collaboration), Deviation from quark number scaling of the anisotropy parameter v_2 of pions, kaons, and protons in $\mathrm{Au}+\mathrm{Au}$ collisions at $\sqrt{s_{NN}}=200$ GeV, Phys. Rev. C **85**, 064914 (2012).
[23] M. Chiu (PHENIX Collaboration), Single spin transverse asymmetries of neutral pions at forward rapidities in $\sqrt{s_{NN}}=62.4$ GeV polarized proton collisions in PHENIX, AIP Conf. Proc. **915**, 539 (2007).
[24] E. Richardson *et al.* (PHENIX Collaboration), A Reaction Plane Detector for PHENIX at RHIC, Nucl. Instrum. Methods Phys. Res., Sect. A **636**, 99 (2011).
[25] A. J. Baltz, C. Chasman, and S. N. White, Correlated forward and backward dissociation and neutron spectra as a luminosity monitor in heavy-ion colliders, Nucl. Instrum. Methods Phys. Res., Sect. A **417**, 1 (1998).
[26] J. Adams *et al.* (STAR Collaboration), Azimuthal Anisotropy and Correlations at Large Transverse Momenta in $p+p$ and $\mathrm{Au}+\mathrm{Au}$ Collisions at $\sqrt{s_{NN}}=200$ GeV, Phys. Rev. Lett. **93**, 252301 (2004).
[27] J. Adams *et al.* (STAR Collaboration), Azimuthal anisotropy in Au+Au collisions at $\sqrt{s_{NN}}=200$ GeV, Phys. Rev. C **72**, 014904 (2005).
[28] A. M. Poskanzer and S. A. Voloshin, Methods for analyzing anisotropic flow in relativistic nuclear collisions, Phys. Rev. C **58**, 1671 (1998).
[29] S. Afanasiev *et al.* (PHENIX Collaboration), Systematic studies of elliptic flow measurements in Au+Au collisions at $\sqrt{s_{NN}}=200$ GeV, Phys. Rev. C **80**, 024909 (2009).
[30] L. Adamczyk *et al.* (STAR Collaboration), Effect of event selection on jetlike correlation measurement in $d+\mathrm{Au}$ collisions at $\sqrt{s_{NN}}=200$ GeV, Phys. Lett. B **743**, 333 (2015).
[31] J. L. Nagle, A. Adare, S. Beckman, T. Koblesky, J. Orjuela Koop, D. McGlinchey, P. Romatschke, J. Carlson, J. E. Lynn, and M. McCumber, Exploiting Intrinsic Triangular Geometry in Relativistic $^3\mathrm{He}+\mathrm{Au}$ Collisions to Disentangle Medium Properties, Phys. Rev. Lett. **113**, 112301 (2014).
[32] P. Romatschke (private communication).
[33] M. Luzum and P. Romatschke, Conformal relativistic viscous hydrodynamics: Applications to RHIC results at $\sqrt{s_{NN}}=200$ GeV, Phys. Rev. C **78**, 034915 (2008).
[34] S. S. Adler *et al.* (PHENIX Collaboration), Elliptic Flow of Identified Hadrons in $\mathrm{Au}+\mathrm{Au}$ Collisions at $\sqrt{s_{NN}}=200$ GeV, Phys. Rev. Lett. **91**, 182301 (2003).
[35] J. Adams *et al.* (STAR Collaboration), Particle Dependence of Azimuthal Anisotropy and Nuclear Modification of Particle Production at Moderate p_T in $\mathrm{Au}+\mathrm{Au}$ Collisions at $\sqrt{s_{NN}}=200$ GeV, Phys. Rev. Lett. **92**, 052302 (2004).
[36] A. Adare *et al.* (PHENIX Collaboration), Scaling Properties of Azimuthal Anisotropy in $\mathrm{Au}+\mathrm{Au}$ and $\mathrm{Cu}+\mathrm{Cu}$ Collisions at $\sqrt{s_{NN}}=200$ GeV, Phys. Rev. Lett. **98**, 162301 (2007).
[37] S. Afanasiev *et al.* (PHENIX Collaboration), Elliptic Flow for ϕ Mesons and (Anti)deuterons in $\mathrm{Au}+\mathrm{Au}$ collisions at $\sqrt{s_{NN}}=200$ GeV, Phys. Rev. Lett. **99**, 052301 (2007).
[38] B. I. Abelev *et al.* (STAR Collaboration), Mass, quark-number, and $\sqrt{s_{NN}}$ dependence of the second and fourth flow harmonics in ultrarelativistic nucleus-nucleus collisions, Phys. Rev. C **75**, 054906 (2007).
[39] B. I. Abelev *et al.* (STAR Collaboration), Centrality dependence of charged hadron and strange hadron elliptic flow from $\sqrt{s_{NN}}=200$ GeV $\mathrm{Au}+\mathrm{Au}$ collisions, Phys. Rev. C **77**, 054901 (2008).
[40] C. Shen, U. W. Heinz, P. Huovinen, and H. Song, Radial and elliptic flow in $\mathrm{Pb}+\mathrm{Pb}$ collisions at the Large Hadron Collider from viscous hydrodynamic, Phys. Rev. C **84**, 044903 (2011).